

# A unified clumped isotope thermometer calibration (0.5–1100°C) using carbonate-based standardization

N.T. Anderson<sup>1\*</sup>, J.R. Kelson<sup>2</sup>, S. Kele<sup>3</sup>, M. Daëron<sup>4</sup>, M. Bonifacie<sup>5</sup>, J. Horita<sup>6</sup>, T.J. Mackey<sup>7</sup>, C.M. John<sup>8</sup>, T. Kluge<sup>9</sup>, P. Petschnig<sup>11</sup>, A.B. Jost<sup>1</sup>, K.W. Huntington<sup>10</sup>, S.M. Bernasconi<sup>11</sup>, K.D. Bergmann<sup>1</sup>

<sup>1</sup>Department of Earth, Atmospheric, and Planetary Sciences, Massachusetts Institute of Technology, Cambridge, MA, 02135

<sup>2</sup>Department of Earth and Environmental Sciences, University of Michigan, Ann Arbor, MI 48109

<sup>3</sup>Institute for Geological and Geochemical Research, Research Centre for Astronomy and Earth Sciences, 1112 Budapest, Hungary

<sup>4</sup>Laboratoire des Sciences du Climat et de l'Environnement, LSCE/IPSL, CEA-CNRS-UVSQ, Université Paris-Saclay, Orme des Merisiers, F-91191, Gif-sur-Yvette Cedex, France

<sup>5</sup>Université de Paris, Institut de Physique du Globe de Paris, CNRS, F-75005 Paris, France

<sup>6</sup>Department of Geosciences, Texas Tech University, Lubbock, TX, 79409

<sup>7</sup>Department of Earth and Planetary Sciences, University of New Mexico, Albuquerque, NM, 87131

<sup>8</sup>Department of Earth Science and Engineering, Imperial College, Prince Consort Rd, London SW7 2AZ

<sup>9</sup>Institute of Applied Geosciences, Karlsruhe Institute of Technology, Adenauerring 20b, 76131 Karlsruhe, Germany

<sup>10</sup>Department of Earth and Space Sciences and Quaternary Research Center, University of Washington, Seattle, WA, USA

<sup>11</sup>Department of Earth Sciences, ETH Zürich, CH8092, Switzerland

## Key Points:

- Reanalysis of previous  $\Delta_{47}$  calibration samples reconciles their discrepancies.
- No statistically significant difference is observed across a wide range of temperature and sample character.
- This  $\Delta_{47}$  calibration is near-identical to recent calcite calibrations using carbonate-based standardization.

\*77 Massachusetts Ave., Cambridge, MA 02139

Corresponding author: N.T. Anderson, [nanderso@mit.edu](mailto:nanderso@mit.edu)

**Abstract**

The potential for carbonate clumped isotope thermometry to independently constrain both the formation temperature of carbonate minerals and fluid oxygen isotope composition allows insight into long-standing questions in the Earth sciences, but remaining discrepancies between calibration schemes hamper interpretation of temperature measurements. To address discrepancies between calibrations, we designed and analyzed a sample suite (41 total samples) with broad applicability across the geosciences, with an exceptionally wide range of formation temperatures, precipitation methods, and mineralogies. We see no statistically significant offset between sample types, although comparison of calcite and dolomite remains inconclusive. When data are reduced identically, the regression defined by this study is nearly identical to that defined by four previous calibration studies that used carbonate-based standardization; we combine these data to present a composite carbonate-standardized regression equation. Agreement across a wide range of temperature and sample types demonstrates a unified, broadly applicable clumped isotope thermometer calibration.

**Plain Language Summary**

Carbonate clumped isotope thermometry is a geochemical tool used to determine the formation temperature of carbonate minerals. In contrast to previous carbonate thermometers, clumped isotope thermometry requires no assumptions about the isotopic composition of the fluid from which the carbonate precipitated. By measuring the clumped isotope composition ( $\Delta_{47}$ ) of carbonate minerals with a known formation temperature, we can construct an empirical calibration for the clumped isotope thermometer that is necessary to convert from a  $\Delta_{47}$  value to formation temperature. Many previous studies have created  $\Delta_{47}$  temperature calibrations, but differences between calibrations have led to large uncertainty in final  $\Delta_{47}$  temperatures. This study measures a large number of samples that span a wide range of temperature (0.5–1100°C) and include many different types of carbonates. These data show that a single calibration equation can describe many sample types, and that when data are carefully standardized to a common set of carbonate materials, calibrations performed at different laboratories agree almost identically. We combine these data to present a carbonate clumped isotope thermometer calibration with broad applicability across the geosciences.

## 1 Introduction

Carbonate clumped isotope thermometry is a powerful geochemical tool that can determine the formation temperature of a carbonate mineral based on the temperature-dependent propensity for  $^{13}\text{C}$ - $^{18}\text{O}$  bond formation in the carbonate crystal lattice (Schauble et al., 2006). By reacting carbonate minerals with acid and measuring the resultant quantity of mass-47  $\text{CO}_2$  molecules ( $\delta^{47}$ ; a value primarily controlled by the abundance of  $^{13}\text{C}$ - $^{18}\text{O}$ - $^{16}\text{O}$  in the analyzed  $\text{CO}_2$ ) and comparing it to a stochastic distribution of mass-47  $\text{CO}_2$  with the same "bulk" isotopic composition ( $\delta^{18}\text{O}$ ,  $\delta^{13}\text{C}$ ), the excess abundance of the doubly substituted isotopologue ( $\Delta_{47}$ ) can be calculated (Ghosh et al., 2006; Schauble et al., 2006). Because  $\Delta_{47}$  reflects an internal state of isotope distribution within the carbonate mineral phase, it can be used to calculate mineral formation temperature ( $T_{\Delta_{47}}$ ) as well as the  $\delta^{18}\text{O}$  of the precipitating fluid. This duo can be leveraged to inform long-standing questions across many geoscience disciplines, including the temperature history of the Earth's oceans, terrestrial paleotemperature, diagenetic history of carbonates, and, when coupled to chronology proxies, basin thermochronology (Finnegan et al., 2011; Snell et al., 2013; Winkelstern & Lohmann, 2016; Lloyd et al., 2017; Mangenot et al., 2018).

The calibration between  $\Delta_{47}$  and carbonate mineral formation temperature is a key intermediary between measurement of  $\text{CO}_2$  gas on a mass spectrometer and calculation of  $T_{\Delta_{47}}$ . Many laboratories have produced  $T$ - $\Delta_{47}$  calibrations since the initial study of Ghosh et al. (2006), spanning various temperatures, mineralogies, precipitation methods, analytical techniques, and data processing procedures (e.g., Ghosh et al., 2006; Huntington et al., 2009; Dennis et al., 2011; Kele et al., 2015; Kelson et al., 2017; Bonifacie et al., 2017; Bernasconi et al., 2018; Jautzy et al., 2020). While early attempts to compare empirical calibration studies across laboratories yielded large discrepancies (e.g., Ghosh et al., 2006; Dennis & Schrag, 2010), recent calibration studies have converged on statistically similar slopes for the  $T$ - $\Delta_{47}$  regression line when data is reduced consistently (Petersen et al., 2019). The convergence of these calibrations is promising, but current discrepancies between empirical calibration equations still lead to  $T_{\Delta_{47}}$  differences of  $\sim 10$  °C for carbonates near Earth surface temperatures and tens of °C for higher temperature samples (Fig. 1; Petersen et al., 2019; Jautzy et al., 2020). Uncertainty from calibrations on this order compounds with analytical uncertainty and hampers interpretation of clumped isotope data.

91 The source of discrepancy between calibration efforts remains unclear. By repro-  
92 cessing past calibration data with a consistent data reduction scheme and IUPAC pa-  
93 rameter set (Brand et al., 2010; Daëron et al., 2016; Schauer et al., 2016), Petersen et  
94 al. (2019) reduced but did not eliminate differences between calibrations. Remaining off-  
95 set in calibration schemes was attributed to one or more of the following: carbon diox-  
96 ide equilibrium scale (CDES) standardization scheme (heated/equilibrated gas vs. carbonate-  
97 based standardization; number, composition, and distribution of standards), differences  
98 in the concentration, temperature, and application method of orthophosphoric acid, sam-  
99 ple gas purification procedures, mass spectrometer methods, pressure baseline correc-  
100 tion, and kinetic isotope effects during carbonate precipitation (Petersen et al., 2019).

101 The 'InterCarb' carbonate clumped isotope inter-laboratory comparison project,  
102 following the principle of equal sample/standard treatment, demonstrated that using car-  
103 bonate standards (as opposed to heated/equilibrated gases) to project raw  $\Delta_{47}$  values  
104 into the 'I-CDES' scale yields reproducibility between 25 laboratories neither greater nor  
105 smaller than predicted based on fully propagating intra-laboratory analytical uncertain-  
106 ties (Bernasconi et al., submitted; Daëron, submitted). Furthermore, the InterCarb study  
107 found that  $\Delta_{47}$  values of measured carbonate standards are statistically indistinguish-  
108 able irrespective of procedural differences between laboratories such as sample gas pu-  
109 rification, mass spectrometer type, or sample acidification procedure. Jautzy et al. (2020)  
110 created a new calibration spanning 5–726°C using carbonate-based standardization, and  
111 found the regression equation defined by the data was statistically indistinguishable from  
112 a series of previous calibration efforts using carbonate-based standardization (Peral et  
113 al., 2018; Bernasconi et al., 2018; Breitenbach et al., 2018; Piasecki et al., 2019; Daëron  
114 et al., 2019; Meinicke et al., 2020). Together, these studies support that varying prepa-  
115 ration and measurement procedures between laboratories produce consistent results if  
116 data are standardized using common carbonate reference materials.

117 Given the promising inter-laboratory consistency of the InterCarb project (Bernasconi  
118 et al., submitted), a new calibration encompassing a spectrum of carbonates relevant to  
119 geoscience researchers that is firmly anchored to the I-CDES using carbonate-based stan-  
120 dardization is required. To ensure that this calibration is applicable across a wide range  
121 of sample material, we reanalyzed a sample suite consisting of natural and synthetic sam-  
122 ples measured from four previously discrepant calibration efforts (Kele et al., 2015; Kluge  
123 et al., 2015; Bonifacie et al., 2017; Kelson et al., 2017) and analyzed a new suite of low-

124 temperature lacustrine carbonates from the Dry Valleys, Antarctica and experimentally  
125 heated carbonate standards. This sample suite spans broad ranges in temperature (0.5  
126 – 1100°C), precipitation method (active degassing, passive degassing, mixed solution, nat-  
127 ural precipitation), mineralogy (calcite, dolomite, and minor aragonite), and initial bulk  
128 isotopic composition. In accordance with the suggestions of the InterCarb project, the  
129 latest anchor values for carbonate standards (ETH-1–4, MERCK, IAEA-C2) were used  
130 for carbonate-based standardization, measurement of each sample was replicated at least  
131 six times (mean = 9), sample to standard ratio was 1:1, IUPAC parameters were used  
132 to correct raw data, and analytical uncertainty and uncertainty associated with creation  
133 of the reference frame was propagated throughout. We compare the regression derived  
134 from data presented here to a suite of previous studies using carbonate-based standard-  
135 ization (recalculated with InterCarb anchor values), and combine these datasets to pro-  
136 pose a unified and broadly applicable clumped isotope thermometer calibration.

## 137 **2 Materials and Methods**

### 138 **2.1 Sample collection and preparation**

139 A total of 41 carbonate samples with known precipitation temperatures from four  
140 previous calibration efforts (Kele et al., 2015; Kluge et al., 2015; Bonifacie et al., 2017;  
141 Kelson et al., 2017), a suite of Antarctic lacustrine carbonate, and a suite of experimen-  
142 tally heated ETH standards were (re)analyzed in this study. Sample formation temper-  
143 ature ranges from 0.5–1100°C. Three samples are stoichiometric dolomite, one sample  
144 is non-stoichiometric proto-dolomite, one sample is aragonite (with minor calcite) and  
145 the remainder are calcite (five with minor aragonite; one with minor goethite).

#### 146 *2.1.1 Natural precipitates*

147 Six calcite samples were collected from three perennially ice-covered lakes in the Dry  
148 Valleys region of Antarctica: two from Lake Fryxell (see Jungblut et al., 2016), three from  
149 Lake Joyce (see Mackey et al., 2018), and one from Lake Vanda (see Mackey et al., 2017).  
150 These carbonates precipitated in association with microbial mats and are shown by pre-  
151 vious work to have extremely low  $\delta^{18}\text{O}$  values of  $-30$  to  $-40\text{‰}$  (Mackey et al., 2018).

152 Ten tufa and travertine deposits were sampled from central Italy, Hungary, Yun-  
153 nan Province (China), Yellowstone (USA), and Tenerife (Spain). Detailed description  
154 of sample localities and strategy are given in Kele et al. (2015) and references therein.

### 155 **2.1.2 Laboratory precipitates**

156 Aliquots of ETH-1 (Carrara marble) and ETH-2 (synthetic carbonate) were heated  
157 to 1100°C and pressurized to 2000 bar for a period of 24 hours at the ETH Zürich Cold  
158 Seal Pressure Vessel Laboratory. Following heating, samples were quenched to room tem-  
159 perature within seconds. See Text S1 in the supporting information for full methods.

160 Fifteen calcite samples from Kelson et al. (2017) were either precipitated with so-  
161 lutions of NaHCO<sub>3</sub> and CaCl<sub>2</sub> or by dissolving CaCO<sub>3</sub> in H<sub>2</sub>O with low pH from CO<sub>2</sub>  
162 bubbling, and then inducing precipitation either through N<sub>2</sub> bubbling or passive degassing.  
163 Carbonic anhydrase was added to four samples. Temperature precision was ±0.5°C.

164 Two calcite samples from Kluge et al. (2015) were precipitated by dissolving CaCO<sub>3</sub>  
165 in H<sub>2</sub>O and letting the solution equilibrate for 2–15 hours, filtering out undissolved car-  
166 bonate, and bubbling N<sub>2</sub> through the solution.

167 Four (proto)dolomite samples used in this study were originally described in Horita  
168 (2014) and Bonifacie et al. (2017). The 80°C sample was precipitated by mixing MgSO<sub>4</sub>,  
169 Ca(NO<sub>3</sub>)<sub>4</sub>H<sub>2</sub>O, and Na<sub>2</sub>CO<sub>3</sub> in a sealed glass bottle for 41 days. The 100, 250, and 350°C  
170 samples were made by mixing ground natural aragonite or calcite with a Ca-Mg-(Na)-  
171 Cl solution and held within 2°C of prescribed value for 6–85 days.

## 172 **2.2 Mass spectrometry**

### 173 **2.2.1 This study**

174 Sample Δ<sub>47</sub> was measured from January 2018 to November 2020 at the MIT Car-  
175 bonate Research Laboratory on a Nu Perspective dual-inlet isotope ratio mass spectrom-  
176 eter with a NuCarb automated sample preparation unit held at 70°C (see Mackey et al.,  
177 2020). Carbonate samples (including dolomite) weighing 400–600 μg reacted for 25 min-  
178 utes in individual glass vials with 150 μl orthophosphoric acid ( $\rho = 1.93 \text{ g/cm}^3$ ). Evolved  
179 CO<sub>2</sub> gas was purified cryogenically and by passive passage through a Porapak trap (1/4"  
180 ID; 0.4 g 50/80 mesh Porapak Q) held at -30°C. Purified sample gas and reference gas

**Table 1.** Description of analyzed and reanalyzed samples.

Study	Mineralogy	Formation	Formation	Samples
			Temp. Range (°C) <sup>a</sup>	Analyzed (this study; orig. study)
Bonifacie et al. (2017)	Dolo., proto-dolo.	Mixed solution	80–350	4; 17
Kele et al. (2015)	Calc. (minor arag.)	Tufa, travertine	5–95	12; 24
Kelson et al. (2017)	Calc. (minor arag.)	Active/passive degas, mixed sol'n	6–78	15; 56
Kluge et al. (2015)	Calc., arag.	Active degas	25–80	2; 29
This study	Calc.	Lacustrine, experimentally heated	0.5–1100	8

<sup>a</sup>Temperature range is only for samples reanalyzed in this study.

181 of known composition were alternately measured on six Faraday collectors ( $m/z$  44–49)  
 182 in 3 acquisitions of 20 cycles, each with 30 second integration time (30 minute total in-  
 183 tegration time). Initial voltage was 8–20 V on the  $m/z$  44 beam with  $2 \times 10^8 \Omega$  resistors  
 184 and depleted by approximately 50% over the course of an analysis. Sample and standard  
 185 gases depleted at equivalent rates from microvolumes over the integration time.

186 Each run of approximately 50 individual analyses began with each of ETH-1–ETH-  
 187 4 in random order, and then alternated between blocks of three unknowns and two ETH  
 188 anchors. Additionally, IAEA-C1, IAEA-C2, and MERCK were respectively measured  
 189 once per run. Unknown to anchor ratio was planned at 1:1 for each run, although gas  
 190 preparation or mass spectrometer error occasionally modified this ratio. The reference  
 191 side of the dual-inlet was refilled with reference gas every 10 to 17 analyses. In total, un-  
 192 knowns were measured 6–16 times over the study interval (362 total unknown analyses).

### 193 2.3 Data processing

194 Raw mass spectrometer data were first processed by removing cycles (i.e., single  
 195 integration cycles) with raw  $\Delta_{47}$  values more than 5 "long-term" standard deviations  
 196 (the mean of the respective cycle-level SD for ETH-1–4 over a 3-month period, 0.10%)  
 197 away from the median  $\Delta_{47}$  measurement for the analysis. Analyses with more than 20  
 198 cycles (out of 60 total cycles) falling outside the 5 long-term SD threshold were removed.

199 In total, 0.81% of cycles and 0.42% of analyses were removed. No pressure baseline cor-  
200 rection was applied. Long-term repeatability (1SD) of  $\Delta_{47}$  for all analyses (after data  
201 processing described above) is 0.036 ‰.

202 After cycle-level outlier removal, data were processed using the 'D47crunch' Python  
203 package (Daëron, submitted) using IUPAC  $^{17}\text{O}$  parameters, 70°C  $^{18}\text{O}$  acid fractionation  
204 factor of 1.00871 (Kim et al., 2007), and projected to the I-CDES with values for ETH-  
205 1–4, IAEA-C2, and MERCK from the InterCarb exercise (Bernasconi et al., submitted),  
206 which uses nominal  $\Delta_{47}$  values for the carbonates determined at an acid reaction tem-  
207 perature of 90°C (0.088‰ lower than values determined at 25°C) after Petersen et al.  
208 (2019). Raw  $\Delta_{47}$  measurements were converted to the I-CDES using a pooled regres-  
209 sion approach that accounts for the relative mapping of all samples in  $\delta^{47}\text{-}\Delta_{47}$  space (Daëron,  
210 submitted). Analytical uncertainty and error associated with creation of the reference  
211 frame were fully propagated through the dataset. A full description of the data reduc-  
212 tion procedure used in D47crunch is detailed in (Daëron, submitted). Each run (typi-  
213 cally 50 analyses) was treated as an analytical session. IAEA-C1 was treated as an un-  
214 known and used as an internal consistency check ( $n = 16$ , mean = 0.292‰, 1SE = 0.098‰).  
215 Finally, Peirce's criterion (Ross, 2003; Zaarur et al., 2013) was applied to the dataset at  
216 the analysis level; a total of six analyses were marked as outliers and removed, followed  
217 by reprocessing of the dataset.

### 218 **3 Results and Discussion**

219 Results for all analyses (re)analyzed here are summarized at the sample level in Ta-  
220 ble 2 (see Dataset S1 and S2 for full results). Accounting for uncertainty in  $\Delta_{47}$  (long-  
221 term repeatability, 1SD) and formation temperature (0.5–10°C) with the regression method  
222 described in York et al. (2004), these data define a linear  $1/T^2\text{-}\Delta_{47}$  relationship from 0.5°C–  
223 1100°C shown in Figure 1.

#### 224 **3.1 Comparison of T- $\Delta_{47}$ relationship across sample types**

225 After applying the 90°C acid fractionation factor of 0.088 ‰ (Petersen et al., 2019),  
226 the published regression equations from Kele et al. (2015); Kluge et al. (2015); Kelson  
227 et al. (2017); Bonifacie et al. (2017) all fall within the 95% confidence interval of the re-  
228 gressions defined by this study's reanalysis of their constituent samples (supporting in-



229 formation Fig. S3). Natural and lab-precipitated samples fall on nearly identical regres-  
230 sion lines (Fig. 2A); analysis of covariance (ANCOVA) fails to reject the null hypoth-  
231 esis that both types of samples are characterized by a single regression line at the 95%  
232 confidence level at our typical sample precision levels (1SE) of  $\sim 10$  ppm ( $p_{slope} = 0.43$ ,  
233  $p_{intercept} = 0.17$ ; see Table S1 in supporting information for full table of ANCOVA anal-  
234 yses). Natural samples display a weaker correlation coefficient ( $r^2 = 0.96$  vs.  $0.99$ ) and  
235 larger error of the estimate, likely due to the greater variability of fluid temperature in  
236 natural settings.

237 Our reanalysis of samples precipitated by Kelson et al. (2017) supports their con-  
238 clusions: we observe no statistically significant  $\Delta_{47}$  offset between passively and actively  
239 degassed samples ( $p_{slope} = 0.19$ ,  $p_{intercept} = 0.79$ ) or with the addition of carbonic an-  
240 hydrase ( $p_{slope} = 0.79$ ,  $p_{intercept} = 0.32$ ; Fig. S1). Reanalysis of samples from Kele et  
241 al. (2015) and Kelson et al. (2017) confirms the conclusions of Kele et al. (2015) that there  
242 is no significant difference between samples precipitated at low ( $< 7$ ) vs. high ( $> 7$ )  
243 pH ( $p_{slope} = 0.4$ ,  $p_{intercept} = 0.99$ ) or intensive vs. moderate precipitation rate ( $p_{slope}$   
244  $= 0.05$ ,  $p_{intercept} = 0.11$ ; Fig. S2). The low number of rapid precipitates (particularly  
245 at low temperatures) makes the above claim inconclusive, but  $\Delta_{47}$  values for two extremely  
246 slow-growing samples re-analyzed for this study at LCSE on an Isoprime 100 mass spec-  
247 trometer (see Text S3), respectively from Devil's Hole, NV, USA, and Laghetto Basso,  
248 Italy (see Winograd et al., 2006; Coplen, 2007; Drysdale et al., 2012; Daëron et al., 2019),  
249 are within 0.001‰ of the expected values based on the calibration from this study (Fig.  
250 3B). Calcite-water fractionation in  $^{18}\text{O}$  calculated from a subset of 20 samples with fluid  
251  $\delta^{18}\text{O}$  data (Fig. S5) agrees closely with the equations of Coplen (2007) and Daëron et  
252 al. (2019). The Antarctic microbially-mediated lacustrine calcites show no discernible  
253 offset from the overall trend, but small sample numbers and limited temperature range  
254 prohibit formal analysis.

255 With only three stoichiometric dolomite samples, no stoichiometric dolomite sam-  
256 ples below  $100^\circ\text{C}$ , and no calcite samples between  $95^\circ\text{C}$  and  $1100^\circ\text{C}$  measured for this  
257 study, we cannot rigorously compare calcite and dolomite regressions; ANCOVA vari-  
258 ably accepts/rejects the null hypothesis depending on categorization of the single protodolomite  
259 sample. Therefore, we cannot assert that dolomite and calcite samples can be described  
260 using a single regression equation, as previously suggested by Bonifacie et al. (2017) and  
261 Petersen et al. (2019); analysis of dolomite samples with lower ( $< 80^\circ\text{C}$ ) and higher ( $>$

262 350°C) formation temperature is needed. The regression through aragonite-containing  
263 samples (four samples < 6%; one sample = 38%; one sample = 78%) is statistically sim-  
264 ilar to the regression through all calcite samples (Fig. 2B). A single sample (Aqua Borra)  
265 with minor goethite (15%) has individual  $\Delta_{47}$  analyses both much higher and lower than  
266 expected, but has a mean  $\Delta_{47}$  value that closely agrees with the regression presented here.

267 The absence of systematic offset in the T- $\Delta_{47}$  relationship corresponding to any  
268 known sample characteristic suggests that discrepancies between these exact samples from  
269 previous calibration efforts are not a function of the character of measured sample ma-  
270 terial (Wacker et al., 2014; Kele et al., 2015; Kluge et al., 2015; Kelson et al., 2017; Boni-  
271 facie et al., 2017). Furthermore, the consistency of the T- $\Delta_{47}$  relationship across a broad  
272 range of materials and temperatures (e.g., from Antarctic lacustrine microbially-mediated  
273 carbonates to laboratory-grown carbonates heated to 1100°C) indicates that a single T-  
274  $\Delta_{47}$  calibration can adequately describe a wide variety of sample types.

### 275 **3.2 Comparison across calibration studies using carbonate-based stan-** 276 **dardization**

277 Reprocessing data from recent calibration studies (Breitenbach et al., 2018; Peral  
278 et al., 2018; Meinicke et al., 2020; Jautzy et al., 2020) with updated InterCarb anchor  
279 values (Bernasconi et al., submitted) yields an almost identical regression to that cal-  
280 culated in this study (Fig. 3). The near-perfect agreement of these calibrations ( $\sim 0.2^\circ\text{C}$   
281 offset near 25°C and 100°C) despite differences in sample material and measurement method  
282 points to the strength of carbonate-based standardization and the potential of a unified  
283 clumped isotope calibration.

284 The clumped isotope calibration reported here covers the broadest range of tem-  
285 peratures, includes diverse carbonates, replicates measurements several times, and uses  
286 a low unknown:anchor ratio to firmly tie unknown measurements to the I-CDES. How-  
287 ever, this calibration has an unequal distribution of samples in  $1/T^2$  space, is anchored  
288 at the coldest temperatures by unusual carbonates, and does not contain marine carbon-  
289 ates, which are of particular interest to the clumped isotope community. To address these  
290 weaknesses, we combine data from this study with four other carbonate-standardized cal-  
291 ibrations (Peral et al., 2018; Meinicke et al., 2020; Jautzy et al., 2020, only cave sam-  
292 ples from Breitenbach et al., 2018) to present a composite  $1/T^2$ - $\Delta_{47}$  regression that has

293 smaller temperature gaps, is anchored at low temperatures by a variety of samples, and  
 294 extends the calibration to biogenic marine carbonates:

$$\Delta_{47(I-CDES90^{\circ}C)} = 0.0390 \pm 0.0004 \times \frac{10^6}{T^2} + 0.154 \pm 0.004 \quad (r^2 = 0.97) \quad (1)$$

295 Along with excellent agreement between laboratories using carbonate-based stan-  
 296 dardization, this dataset and the community-developed InterCarb anchor values (Bernasconi  
 297 et al., submitted) narrow the discrepancy between calibrations using carbonate anchor  
 298 values and heated/equilibrated gases, most notably Petersen et al. (2019). Specifically,  
 299 calibrations of Jautzy et al. (2020) and Petersen et al. (2019) differed by 5°C near 25°C  
 300 and 20°C near 100°C; the composite calibration regression shown in Equation 1 differs  
 301 from Petersen et al. (2019) by 3°C near 25°C and by 7°C near 100°C (Fig. 1A).

### 302 **3.3 Non-linearity of $1/T^2$ - $\Delta_{47}$ relationship for high-temperature pre-** 303 **cipitates**

304 At high temperatures, theory predicts a non-linear  $1/T^2$ - $\Delta_{47}$  relationship (e.g., Guo  
 305 et al., 2009; Hill et al., 2014), supported by recent empirical calibrations (e.g., Müller  
 306 et al., 2019; Jautzy et al., 2020). A third-order polynomial regression through our data  
 307 falls within the 95% CL of our linear fit over the entire temperature range (Fig. 3A) and  
 308 does not improve the goodness of fit ( $r^2 = 0.97$  for both); we observe no evidence that  
 309 a non-linear fit better describes high-temperature data.

## 310 **4 Conclusions**

311 When measured in a consistent analytical setting with carbonate-based standard-  
 312 ization, no systematic offset is observed between samples precipitated across a broad spec-  
 313 trum of conditions that were previously determined to have disparate  $\Delta_{47}$  values. Among  
 314 sample types measured here, we find no evidence that the particular character of sam-  
 315 ple material (e.g., mineralogy, addition of carbonic anhydrase, pH, precipitation rate, bi-  
 316 ological mediation) influences the  $\Delta_{47}$  calibration, although calcite and dolomite agree-  
 317 ment remain inconclusive.

318 Furthermore, when anchor values from the InterCarb exercise (Bernasconi et al.,  
 319 submitted) are used with data reduction best practices (Petersen et al., 2019; Daëron,

**Table 2.** Final corrected  $\delta^{13}\text{C}_{VPDB}$  (‰),  $\delta^{18}\text{O}_{VSMOW}$  (‰), and  $\Delta_{47(CDES90^\circ\text{C})}$  (‰) results.

Sample name	Author	Mineralogy	Method	T(°C)	N	$\delta^{13}\text{C}$	$\delta^{18}\text{O}$	$\Delta_{47}$	SE	95% CL
IPGP_100-A3	Bonifacie	Dolomite	Lab	102.3	9	-46.3	-17.4	0.427	0.015	0.029
IPGP_250-A5	Bonifacie	Dolomite	Lab	252.1	9	-52.8	-28.0	0.275	0.025	0.049
IPGP_350-A9	Bonifacie	Dolomite	Lab	351.4	10	-55.6	-32.0	0.232	0.018	0.035
IPGP_80-1	Bonifacie	Proto-dolo.	Lab	80.2	10	-6.9	-16.2	0.495	0.012	0.024
ETH-1-1100-SAM	This study	Calcite	Lab	1100	10	2.0	-2.0	0.178	0.018	0.036
ETH-2-1100-SAM	This study	Calcite	Lab	1100	10	-10.1	-18.4	0.192	0.017	0.034
HT_25C	Kluge	Calcite	Lab	25	9	2.1	-6.2	0.610	0.013	0.026
HT_80C	Kluge	Aragonite	Lab	80	9	1.1	-15.4	0.487	0.013	0.025
AQUA_BORRA	Kele	Calcite	Natural	36.1	11	1.7	-8.4	0.577	0.012	0.023
BUK_4	Kele	Calcite	Natural	54.9	9	2.2	-15.0	0.541	0.013	0.025
CANARIAN	Kele	Calcite	Natural	33.8	8	0.1	-10.2	0.584	0.014	0.027
CANNATOPA	Kele	Calcite	Natural	11	8	-4.1	-5.4	0.628	0.014	0.027
IGAL	Kele	Calcite	Natural	75	10	0.6	-13.5	0.475	0.012	0.024
LAPIGNA	Kele	Calcite	Natural	12.5	9	-11.4	-5.5	0.621	0.013	0.026
NG_2	Kele	Calcite	Natural	60.4	9	3.6	-24.6	0.505	0.013	0.025
P5_SUMMER	Kele	Calcite	Natural	12	9	5.4	-14.3	0.633	0.013	0.026
P5_WINTER	Kele	Calcite	Natural	5	10	5.1	-12.7	0.635	0.013	0.026
SARTEANO	Kele	Calcite	Natural	20.7	9	0.4	-7.3	0.594	0.013	0.025
SZAL-2	Kele	Calcite	Natural	11	9	-10.3	-8.2	0.654	0.013	0.026
TURA	Kele	Calcite	Natural	95	9	3.7	-23.2	0.409	0.013	0.025
LF2012-9-7-A	This study	Calcite	Natural	2.5	4	2.6	-27.2	0.663	0.023	0.045
LF2012-D1-A	This study	Calcite	Natural	2.5	4	3.4	-27.1	0.658	0.023	0.044
LJ2010-12A-Z1A	This study	Calcite	Natural	0.5	13	7.7	-39.4	0.668	0.014	0.028
LJ2010-12A-Z2A	This study	Calcite	Natural	0.5	6	8.1	-38.1	0.672	0.020	0.039
LJ2010-5B-A	This study	Calcite	Natural	0.5	11	8.1	-37.6	0.676	0.014	0.027
LV26NOV10-2A	This study	Calcite	Natural	4	6	11.2	-29.0	0.652	0.018	0.035
UWCP14.20C.9	Kelson	Calcite	Lab	23	8	-21.1	-10.8	0.604	0.014	0.028
UWCP14.20C_CA.11	Kelson	Calcite	Lab	23	10	-14.1	-10.9	0.615	0.013	0.025
UWCP14.21C.1	Kelson	Calcite	Lab	22	8	-18.6	-11.1	0.611	0.014	0.028
UWCP14.4C.3	Kelson	Calcite	Lab	6	8	-21.3	-6.6	0.650	0.014	0.028
UWCP14.4C.4	Kelson	Calcite	Lab	6	9	-23.4	-6.7	0.658	0.013	0.026
UWCP14.50C.2	Kelson	Calcite	Lab	51	9	-18.4	-16.4	0.534	0.013	0.026
UWCP14.50C.7	Kelson	Calcite	Lab	54	9	-0.2	-17.4	0.518	0.013	0.025
UWCP14.50C_CA.11	Kelson	Calcite	Lab	50	9	-18.5	-15.9	0.527	0.014	0.027
UWCP14.60C.2	Kelson	Calcite	Lab	66	9	-12.5	-18.2	0.491	0.013	0.026
UWCP14.70C.4	Kelson	Calcite	Lab	72	8	-17.7	-18.8	0.490	0.014	0.028
UWCP14.70C_CA.4	Kelson	Calcite	Lab	71	9	-0.2	-19.6	0.493	0.013	0.025
UWCP14.80C.2	Kelson	Calcite	Lab	78	9	-6.9	-20.9	0.483	0.013	0.025
UWCP14.8C.2	Kelson	Calcite	Lab	9	9	-15.1	-7.7	0.633	0.013	0.026
UWCP14.8C.6	Kelson	Calcite	Lab	9	9	0.4	-8.8	0.648	0.013	0.026
UWCP14.8C_CA.4	Kelson	Calcite	Lab	9	8	-17.4	-8.1	0.648	0.014	0.028

320 submitted), the  $1/T^2$ - $\Delta_{47}$  regression defined by data presented here is nearly identical  
321 (0.2°C offset at 25°C and 100°C) to the regression defined by a suite of recent calibra-  
322 tion studies (Peral et al., 2018; Breitenbach et al., 2018; Meinicke et al., 2020; Jautzy  
323 et al., 2020) and closely approximates the composite calibration of Petersen et al. (2019).  
324 Equation 1 spans the broadest range of temperatures measured in a consistent analyt-  
325 ical setting and, when corrected with carbonate anchor values from the InterCarb ex-  
326 ercise (Bernasconi et al., submitted) or heated/equilibrated gases, may be applied across  
327 a wide range of natural and laboratory-grown carbonate material.

### 328 **Acknowledgments**

329 Regression equations from previous publications are included in cited papers. Sample  
330 and replicate level data are included in this manuscript in the supporting information  
331 and will be archived in the EarthChem database using a data template specifically de-  
332 signed for carbonate clumped isotope data (Petersen et al., 2019) pending acceptance  
333 of this manuscript; reprocessed data from Peral et al. (2018); Breitenbach et al. (2018);  
334 Meinicke et al. (2020); ? (?) will be archived in the EarthChem database. N.T. Ander-  
335 son acknowledges the support of the J.H. and E.V. Wade Fellowship and the mTerra Cat-  
336 alyst Fund. Members of the Bergmann Lab (Marjorie Cantine, Athena Eyster, Sam Gold-  
337 berg, and Julia Wilcots) provided helpful feedback on early drafts. K. Bergmann acknowl-  
338 edges support from the Packard Foundation, NASA Exobiology Grant 80NSSC19K0464  
339 and the MIT Wade Fund.

### 340 **References**

- 341 Bernasconi, S. M., Daëron, M., Bergmann, K. D., Bonifacie, M., Meckler, A. N.,  
342 Affek, H. P., ... Ziegler, M. (submitted). InterCarb: A community effort to  
343 improve inter-laboratory standardization of the carbonate clumped isotope  
344 thermometer using carbonate standards. *Geochemistry, Geophysics, Geosys-*  
345 *tems*. doi: 10.1002/essoar.10504430.4
- 346 Bernasconi, S. M., Müller, I. A., Bergmann, K. D., Breitenbach, S. F., Fernan-  
347 dez, A., Hodell, D. A., ... Ziegler, M. (2018). Reducing uncertainties in  
348 carbonate clumped isotope analysis through consistent carbonate-based stan-  
349 dardization. *Geochemistry, Geophysics, Geosystems*, 19(9), 2895–2914. doi:  
350 10.1029/2017GC007385

- 351 Bonifacie, M., Calmels, D., Eiler, J. M., Horita, J., Chaduteau, C., Vasconcelos, C.,  
352 ... Bourrand, J. J. (2017). Calibration of the dolomite clumped isotope ther-  
353 mometer from 25 to 350 C, and implications for a universal calibration for all  
354 (Ca, Mg, Fe)CO<sub>3</sub> carbonates. *Geochimica et Cosmochimica Acta*, 200, 255–279.  
355 doi: 10.1016/j.gca.2016.11.028
- 356 Brand, W. A., Assonov, S. S., & Coplen, T. B. (2010). Correction for the 17O  
357 interference in  $\delta^{13}\text{C}$  measurements when analyzing CO<sub>2</sub> with stable isotope  
358 mass spectrometry (IUPAC Technical Report). *Pure Applied Chemistry*, 82(8),  
359 1719–1733. doi: 10.1351/PAC-REP-09-01-05
- 360 Breitenbach, S. F., Mleneck-Vautravers, M. J., Grauel, A. L., Lo, L., Bernasconi,  
361 S. M., Müller, I. A., ... Hodell, D. A. (2018). Coupled Mg/Ca and  
362 clumped isotope analyses of foraminifera provide consistent water temper-  
363 atures. *Geochimica et Cosmochimica Acta*, 236, 283–296. doi: 10.1016/  
364 j.gca.2018.03.010
- 365 Coplen, T. B. (2007). Calibration of the calcite-water oxygen-isotope geothermome-  
366 ter at Devils Hole, Nevada, a natural laboratory. *Geochimica et Cosmochimica*  
367 *Acta*, 71(16), 3948–3957. doi: 10.1016/j.gca.2007.05.028
- 368 Daëron, M. (submitted). Full propagation of analytical uncertainties in D47  
369 measurements. *Geochemistry, Geophysics, Geosystems*. doi: 10.1002/  
370 essoar.10504430.4
- 371 Daëron, M., Blamart, D., Peral, M., & Affek, H. P. (2016). Absolute isotopic abun-  
372 dance ratios and the accuracy of  $\Delta 47$  measurements. *Chemical Geology*, 442,  
373 83–96. doi: 10.1016/j.chemgeo.2016.08.014
- 374 Daëron, M., Drysdale, R. N., Peral, M., Huyghe, D., Blamart, D., Coplen,  
375 T. B., ... Zanchetta, G. (2019). Most Earth-surface calcites precipitate  
376 out of isotopic equilibrium. *Nature Communications*, 10(1), 1–7. doi:  
377 10.1038/s41467-019-08336-5
- 378 Dennis, K. J., Affek, H. P., Passey, B. H., Schrag, D. P., & Eiler, J. M. (2011).  
379 Defining an absolute reference frame for clumped' isotope studies of  
380 CO<sub>2</sub>. *Geochimica et Cosmochimica Acta*, 75(22), 7117–7131. Retrieved  
381 from <http://dx.doi.org/10.1016/j.gca.2011.09.025> doi: 10.1016/  
382 j.gca.2011.09.025
- 383 Dennis, K. J., & Schrag, D. P. (2010). Clumped isotope thermometry of carbon-

- 384 atites as an indicator of diagenetic alteration. *Geochimica et Cosmochimica*  
385 *Acta*, *74*(14), 4110–4122. doi: 10.1016/j.gca.2010.04.005
- 386 Drysdale, R. N., Paul, B. T., Hellstrom, J. C., Couchoud, I., Greig, A., Bajo, P.,  
387 ... Woodhead, J. D. (2012). Precise microsampling of poorly laminated  
388 speleothems for U-series dating. *Quaternary Geochronology*, *14*, 38–47. doi:  
389 10.1016/j.quageo.2012.06.009
- 390 Finnegan, S., Bergmann, K., Eiler, J. M., Jones, D. S., Fike, D. A., Eisenman,  
391 I., ... Fischer, W. W. (2011). The magnitude and duration of Late  
392 Ordovician-Early Silurian glaciation. *Science*, *331*(6019), 903–906. doi:  
393 10.1126/science.1200803
- 394 Ghosh, P., Adkins, J., Affek, H., Balta, B., Guo, W., Schauble, E. A., ... Eiler,  
395 J. M. (2006).  $^{13}\text{C}$ - $^{18}\text{O}$  bonds in carbonate minerals: A new kind of pale-  
396 othermometer. *Geochimica et Cosmochimica Acta*, *70*(6), 1439–1456. doi:  
397 10.1016/j.gca.2005.11.014
- 398 Guo, W., Mosenfelder, J. L., Goddard, W. A., & Eiler, J. M. (2009). Isotopic  
399 fractionations associated with phosphoric acid digestion of carbonate miner-  
400 als: Insights from first-principles theoretical modeling and clumped isotope  
401 measurements. *Geochimica et Cosmochimica Acta*, *73*(24), 7203–7225. doi:  
402 10.1016/j.gca.2009.05.071
- 403 Hill, P. S., Tripathi, A. K., & Schauble, E. A. (2014). Theoretical constraints  
404 on the effects of pH, salinity, and temperature on clumped isotope sig-  
405 natures of dissolved inorganic carbon species and precipitating carbon-  
406 ate minerals. *Geochimica et Cosmochimica Acta*, *125*, 610–652. doi:  
407 10.1016/j.gca.2013.06.018
- 408 Horita, J. (2014). Oxygen and carbon isotope fractionation in the system dolomite-  
409 water-CO<sub>2</sub> to elevated temperatures. *Geochimica et Cosmochimica Acta*, *129*,  
410 111–124. doi: 10.1016/j.gca.2013.12.027
- 411 Huntington, K. W., Eiler, J. M., Affek, H. P., Guo, W., Bonifacie, M., Yeung, L. Y.,  
412 ... Came, R. (2009). Methods and limitations of 'clumped' CO<sub>2</sub> isotope  
413 ( $\Delta 47$ ) analysis by gas-source isotope ratiomass spectrometry. *Journal of Mass*  
414 *Spectrometry*, *44*(9), 1318–1329. doi: 10.1002/jms.1614
- 415 Jautzy, J., Savard, M., Dhillon, R., Bernasconi, S., Lavoie, D., & Smirnov, A.  
416 (2020). Clumped isotope temperature calibration for calcite: Bridging the

- 417 ory and experimentation. *Geochemical Perspective Letters*, 14, 36–41. doi:  
418 10.7185/geochemlet.2021
- 419 Jungblut, A. D., Hawes, I., Mackey, T. J., Krusor, M., Doran, P. T., Sumner, D. Y.,  
420 ... Goroncy, A. K. (2016). Microbial mat communities along an oxygen gra-  
421 dient in a perennially ice-covered Antarctic lake. *Applied and Environmental*  
422 *Microbiology*, 82(2), 620–630. doi: 10.1128/AEM.02699-15
- 423 Kele, S., Breitenbach, S. F., Capezzuoli, E., Meckler, A. N., Ziegler, M., Millan,  
424 I. M., ... Bernasconi, S. M. (2015). Temperature dependence of oxygen- and  
425 clumped isotope fractionation in carbonates: A study of travertines and tufas  
426 in the 6-95C temperature range. *Geochimica et Cosmochimica Acta*, 168,  
427 172–192. doi: 10.1016/j.gca.2015.06.032
- 428 Kelson, J. R., Huntington, K. W., Schauer, A. J., Saenger, C., & Lechler, A. R.  
429 (2017). Toward a universal carbonate clumped isotope calibration: Di-  
430 verse synthesis and preparatory methods suggest a single temperature  
431 relationship. *Geochimica et Cosmochimica Acta*, 197, 104–131. doi:  
432 10.1016/j.gca.2016.10.010
- 433 Kim, S. T., Mucci, A., & Taylor, B. E. (2007). Phosphoric acid fractionation fac-  
434 tors for calcite and aragonite between 25 and 75C: Revisited. *Chemical Geol-*  
435 *ogy*, 246(3-4), 135–146. doi: 10.1016/j.chemgeo.2007.08.005
- 436 Kluge, T., John, C. M., Jourdan, A. L., Davis, S., & Crawshaw, J. (2015). Labora-  
437 tory calibration of the calcium carbonate clumped isotope thermometer in the  
438 25-250C temperature range. *Geochimica et Cosmochimica Acta*, 157, 213–227.  
439 doi: 10.1016/j.gca.2015.02.028
- 440 Lloyd, M. K., Eiler, J. M., & Nabelek, P. I. (2017). Clumped isotope thermometry  
441 of calcite and dolomite in a contact metamorphic environment. *Geochimica et*  
442 *Cosmochimica Acta*, 197, 323–344. doi: 10.1016/j.gca.2016.10.037
- 443 Mackey, T. J., Jost, A. B., Creveling, J. R., & Bergmann, K. D. (2020). A Decrease  
444 to Low Carbonate Clumped Isotope Temperatures in Cryogenian Strata. *AGU*  
445 *Advances*, 1(3). doi: 10.1029/2019av000159
- 446 Mackey, T. J., Sumner, D. Y., Hawes, I., & Jungblut, A. D. (2017). Morpholog-  
447 ical signatures of microbial activity across sediment and light microenviron-  
448 ments of Lake Vanda, Antarctica. *Sedimentary Geology*, 361, 82–92. doi:  
449 10.1016/j.sedgeo.2017.09.013



- 450 Mackey, T. J., Sumner, D. Y., Hawes, I., Leidman, S. Z., Andersen, D. T., & Jung-  
451 blut, A. D. (2018). Stromatolite records of environmental change in perennially  
452 ice-covered Lake Joyce, McMurdo Dry Valleys, Antarctica. *Biogeochemistry*,  
453 *137*(1-2), 73–92. doi: 10.1007/s10533-017-0402-1
- 454 Mangenot, X., Gasparrini, M., Gerdes, A., Bonifacie, M., & Rouchon, V. (2018). An  
455 emerging thermochronometer for carbonate-bearing rocks:  $\Delta 47$  /(U-Pb). *Geol-*  
456 *ogy*, *46*(12), 1067–1070. doi: 10.1130/G45196.1
- 457 Meinicke, N., Ho, S. L., Hannisdal, B., Nürnberg, D., Tripathi, A., Schiebel, R., &  
458 Meckler, A. N. (2020). A robust calibration of the clumped isotopes to tem-  
459 perature relationship for foraminifers. *Geochimica et Cosmochimica Acta*, *270*,  
460 160–183. doi: 10.1016/j.gca.2019.11.022
- 461 Müller, I. A., Rodriguez-Blanco, J. D., Storck, J.-C., Santilli, G., Bontognali,  
462 T. R. R., Vasconcelos, C., ... Bernasconi, S. M. (2019). Calibration of  
463 the oxygen and clumped isotope thermometers for (proto-) dolomite based  
464 on synthetic and natural carbonates. *Chemical Geology*, *525*, 1–17. doi:  
465 10.1016/j.chemgeo.2019.07.014
- 466 Peral, M., Daëron, M., Blamart, D., Bassinot, F., Dewilde, F., Smialkowski, N., ...  
467 Waelbroeck, C. (2018). Updated calibration of the clumped isotope thermome-  
468 ter in planktonic and benthic foraminifera. *Geochimica et Cosmochimica Acta*,  
469 *239*, 1–16. doi: 10.1016/j.gca.2018.07.016
- 470 Petersen, S. V., Defliese, W. F., Saenger, C., Daëron, M., Huntington, K. W.,  
471 John, C. M., ... Winkelstern, I. Z. (2019). Effects of improved  $^{17}\text{O}$  cor-  
472 rection on interlaboratory agreement in clumped isotope calibrations, esti-  
473 mates of mineral-specific offsets, and temperature dependence of acid diges-  
474 tion fractionation. *Geochemistry, Geophysics, Geosystems*, 3495–3519. doi:  
475 10.1029/2018gc008127
- 476 Piasecki, A., Bernasconi, S. M., Grauel, A. L., Hannisdal, B., Ho, S. L., Leutert,  
477 T. J., ... Meckler, N. (2019). Application of clumped isotope thermome-  
478 try to benthic foraminifera. *Geochemistry, Geophysics, Geosystems*, *20*(4),  
479 2082–2090. doi: 10.1029/2018GC007961
- 480 Ross, S. (2003). Peirce’s criterion for the elimination of suspect experimental data.  
481 *Journal of Engineering Technology*, *20*, 1–12.
- 482 Schauble, E. A., Ghosh, P., & Eiler, J. M. (2006). Preferential formation of

- 483 13C 18O bonds in carbonate minerals, estimated using first-principles lat-  
484 tice dynamics. *Geochimica et Cosmochimica Acta*, 70(10), 2510–2529. doi:  
485 10.1016/j.gca.2006.02.011
- 486 Schauer, A. J., Kelson, J., Saenger, C., & Huntington, K. W. (2016). Choice of  
487 17O correction affects clumped isotope ( $\Delta 47$ ) values of CO<sub>2</sub> measured with  
488 mass spectrometry. *Rapid Communications in Mass Spectrometry*, 30(24),  
489 2607–2616. doi: 10.1002/rcm.7743
- 490 Snell, K. E., Thrasher, B. L., Eiler, J. M., Koch, P. L., Sloan, L. C., & Tabor, N. J.  
491 (2013). Hot summers in the Bighorn Basin during the early Paleogene. *Geol-*  
492 *ogy*, 41(1), 55–58. doi: 10.1130/G33567.1
- 493 Wacker, U., Fiebig, J., Tödter, J., Schöne, B. R., Bahr, A., Friedrich, O., ...  
494 Joachimski, M. M. (2014). Empirical calibration of the clumped isotope pale-  
495 othermometer using calcites of various origins. *Geochimica et Cosmochimica*  
496 *Acta*, 141, 127–144. Retrieved from 10.1016/j.gca.2014.06.004
- 497 Winkelstern, I. Z., & Lohmann, K. C. (2016). Shallow burial alteration of dolomite  
498 and limestone clumped isotope geochemistry. *Geology*, 44(6), 467–470. doi: 10  
499 .1130/G37809.1
- 500 Winograd, I. J., Landwehr, J. M., Coplen, T. B., Sharp, W. D., Riggs, A. C., Lud-  
501 wig, K. R., & Kolesar, P. T. (2006). Devils Hole, Nevada,  $\delta 18\text{O}$  record ex-  
502 tended to the mid-Holocene. *Quaternary Research*, 66(2), 202–212. doi:  
503 10.1016/j.yqres.2006.06.003
- 504 York, D., Evensen, N. M., López, M., & Delgado, J. D. B. (2004). Unified equations  
505 for the slope, intercept, and standard errors of the best straight line. *American*  
506 *Journal of Physics*, 72(3), 367–373. doi: 10.1119/1.1632486
- 507 Zaarur, S., Affek, H. P., & Brandon, M. T. (2013). A revised calibration of the  
508 clumped isotope thermometer. *Earth and Planetary Science Letters*, 382, 47–  
509 57. Retrieved from <http://dx.doi.org/10.1016/j.epsl.2013.07.026> doi:  
510 10.1016/j.epsl.2013.07.026

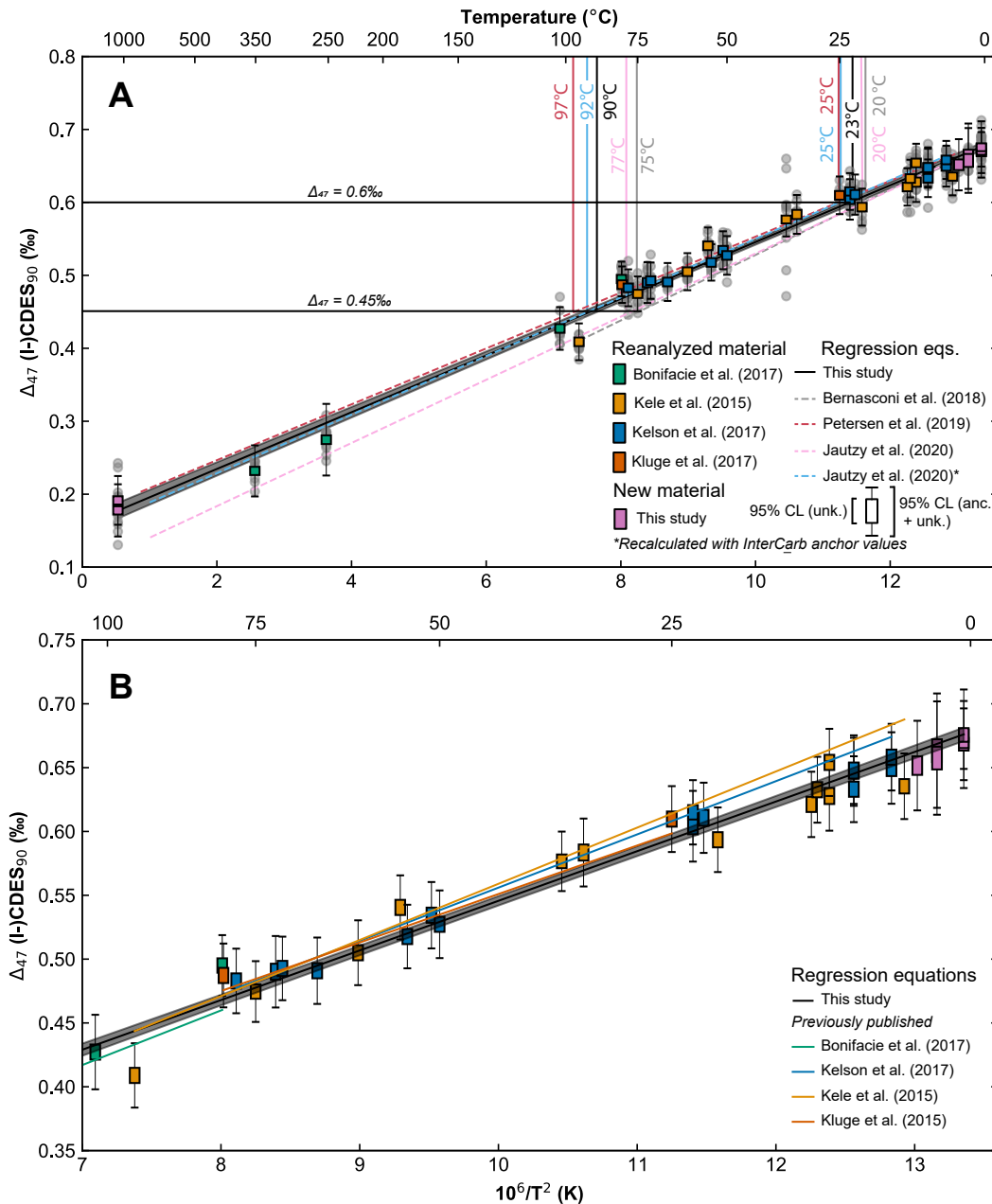


**Figure 1.** A. Linear  $1/T^2$ - $\Delta_{47}$  regression and 95% confidence interval (York et al., 2004) for samples (re)analyzed in this study shown with recently published calibrations. Solid vertical lines show approximate formation temperature for each calibration when  $\Delta_{47} = 0.45\text{‰}$  and  $\Delta_{47} = 0.6\text{‰}$ . Error bars correspond to 95% confidence limits accounting for error from unknown and anchor analyses; boxes correspond to 95% CL not accounting for normalization errors; gray circles show individual analyses. The regression from this study is nearly identical to the regression from Jautzy et al. (2020) when all  $\Delta_{47}$  values are calculated with 'InterCarb' (Bernasconi et al., submitted) anchor values. B. T- $\Delta_{47}$  relationship for samples 0–100°C including regressions from studies with material reanalyzed for this study (Bonifacie et al. (2017), Eq. 1; Kele et al. (2015), Eq. 1; Kelson et al. (2017) Eq. 1; Kluge et al. (2015), Table 1, 'This study, linear fit'; all converted to 90°C acid temperature using AFF<sup>-19</sup> values from Petersen et al., 2019).

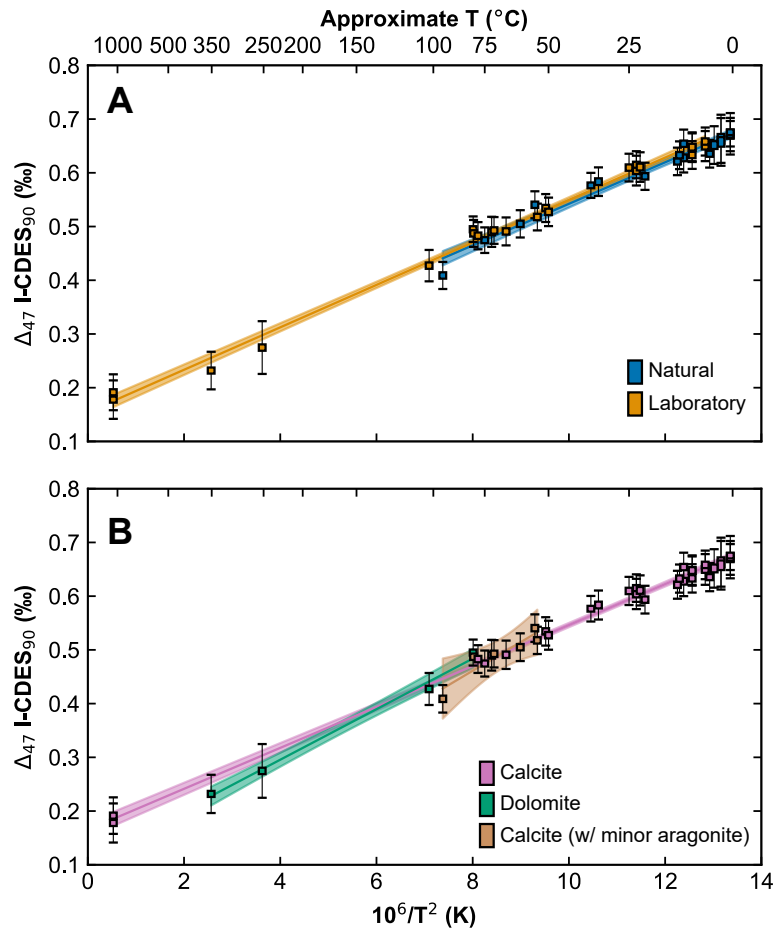
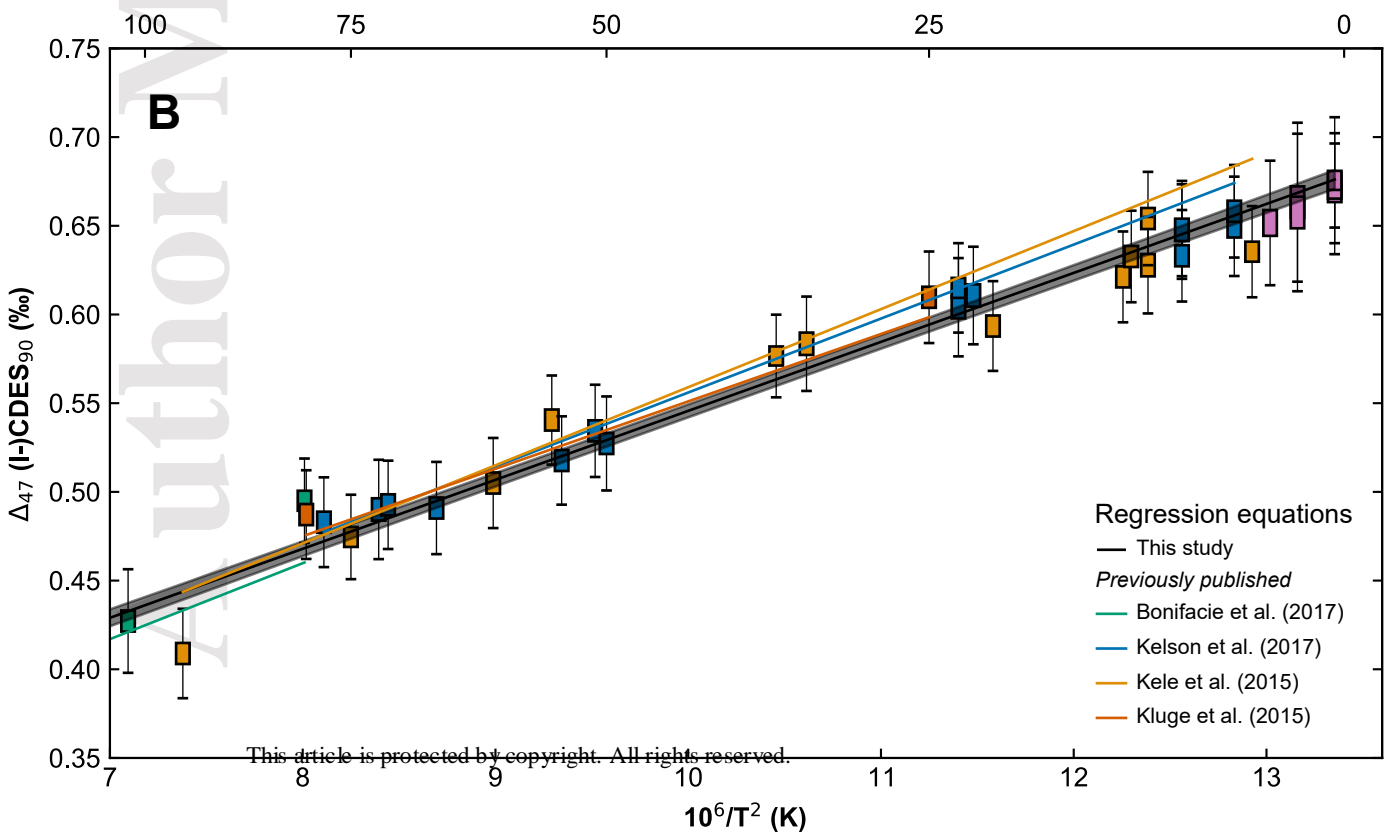
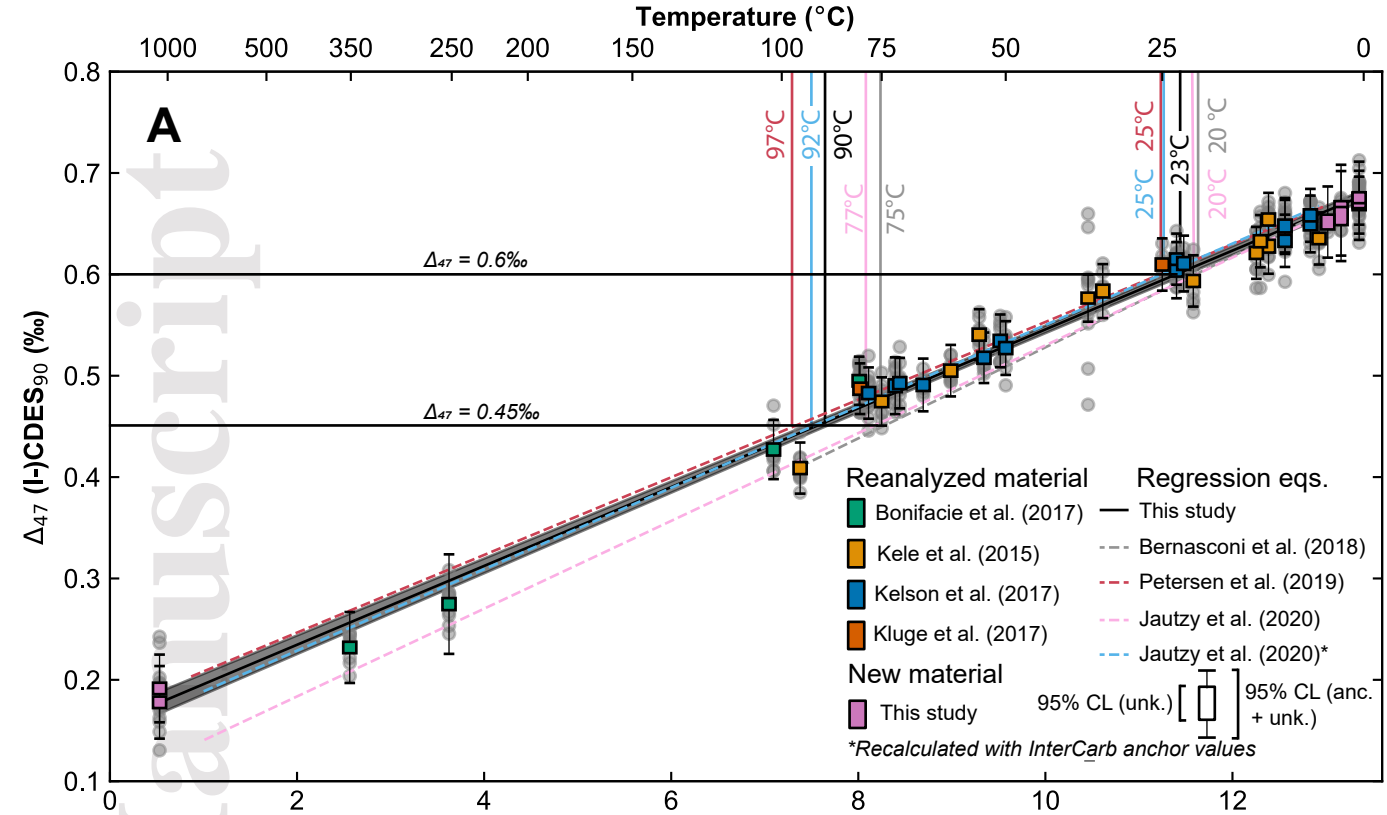


**Figure 2.** A.  $1/T^2$ - $\Delta_{47}$  comparison of natural and laboratory precipitated sample material. Error bars correspond to 95% confidence limits accounting for error from both unknown and anchor analyses; boxes correspond to 95% CL not accounting for normalization errors. Natural samples have larger uncertainty of the estimate and a poorer fit, likely due to natural variability in formation temperature and a smaller temperature range. B. Comparison of calcite, (proto)dolomite, and aragonite sample material. The regression lines between calcite and dolomite diverge but 95% confidence intervals overlap; divergence of regression equations may be related to the small temperature range of dolomite (relative to calcite) measured in this study and the small number of dolomite samples.



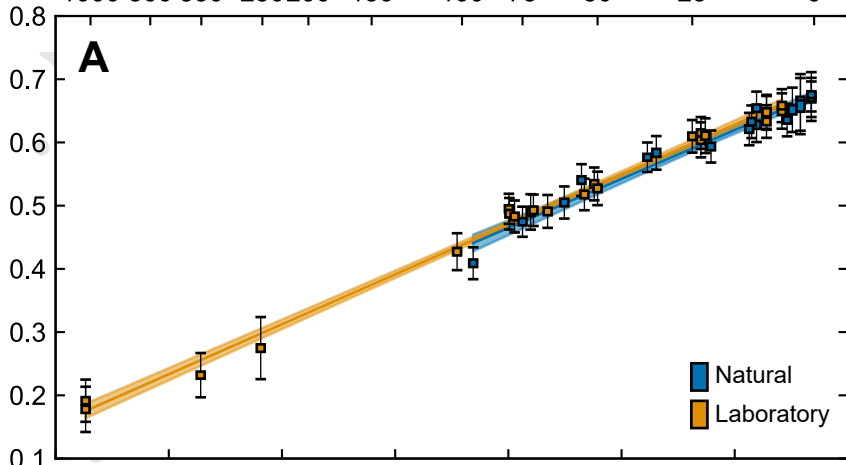


Approximate T (°C)

1000 500 350 250 200 150 100 75 50 25 0

**A**

$\Delta_{47}$  I-CDES<sub>90</sub> (‰)



**B**

$\Delta_{47}$  I-CDES<sub>90</sub> (‰)

